Apoptosis (2019) 24:934–945
https://doi.org/10.1007/s10495-019-01571-7

Liver-specific Bid silencing inhibits APAP-induced cell death in mice

Mareike Maxa[1] · Ute Schaeper[2] · Sibylle Dames[2] · Brigitte Vollmar[1] · Angela Kuhla[1]

Published online: 1 October 2019

Abstract
Acetaminophen (APAP)-induced acute liver failure (ALF) is a life-threatening disease with only a few treatment options available. Though extensive research has been conducted for more than 40 years, the underlying pathomechanisms are not completely understood. Here, we studied as to whether APAP-induced ALF can be prevented in mice by silencing the BH3-interacting domain death agonist (Bid) as a potential key player in APAP pathology. For silencing Bid expression in mice, $siRNA^{Bid}$ was formulated with the liver-specific siRNA delivery system DBTC and administered 48 h prior to APAP exposure. Mice which were pre-treated with HEPES ($vehicle^{HEPES}$) and $siRNA^{Luci}$ served as siRNA controls. Hepatic pathology was assessed by in vivo fluorescence microscopy, molecular biology, histology and laboratory analysis 6 h after APAP or PBS exposure. Application of $siRNA^{Bid}$ caused a significant decrease of mRNA and protein expression of Bid in APAP-exposed mice. Off-targets, such as cytochrome P450 2E1 and glutathione, which are known to be consumed under APAP intoxication, were comparably reduced in all APAP-exposed mice, underlining the specificity of Bid silencing. In APAP-exposed mice non-sterile inflammation with leukocyte infiltration and perfusion failure remained almost unaffected by Bid silencing. However, the Bid silencing reduced hepatocellular damage, evident by a remarkable decrease of DNA fragmented cells in APAP-exposed mice. In these mice, the expression of the pro-apoptotic protein Bax, which recently gained importance in the cell death pathway of regulated necrosis, was also significantly reduced, in line with a decrease in both, necrotic liver tissue and plasma transaminase activities. In addition, plasma levels of HMGB1, a marker of sterile inflammation, were significantly diminished. In conclusion, the liver-specific silencing of Bid expression did not protect APAP-exposed mice from microcirculatory dysfunction, but markedly protected the liver from necrotic cell death and in consequence from sterile inflammation. The study contributes to the understanding of the molecular mechanism of the APAP-induced pathogenic pathway by strengthening the importance of Bid and Bid silencing associated effects.

Keywords Acetaminophen · Necrosis · Apoptosis · siRNA · DBTC lipoplex · BH3-interacting domain death agonist

Introduction

Acute liver failure (ALF) is a clinical syndrome characterized by peripheral vasodilation, encephalopathy and coagulopathy culminating in multi-organ dysfunction and death [1]. There are two main causes for ALF in Europe: hepatitis and medical intoxication [2, 3]. In the USA and other western countries the most frequent cause for ALF with about 40% is the acetaminophen (acetyl-para-aminophenol, APAP)—intoxication [2, 4–7]. Especially, the combination of drugs with APAP leads to an unintentional and chronic APAP overdose [8].

The pathomechanisms of APAP are still not completely understood [9–15]. It is widely accepted that APAP is metabolized in the liver by cytochrome P450 family to *N*-acetyl-p-benzoquinone (NAPQI), which consumes glutathione [12]. When this pathway is saturated, NAPQI generates covalent protein adducts especially on mitochondrial proteins and leads to mitochondrial dysfunction [12, 16–18]. These protein adducts seem to be the most relevant cause for APAP toxicity [19–21]. Further, a sterile inflammation and also a perfusion deficit are described [22, 23], which may lead to

Electronic supplementary material The online version of this article (https://doi.org/10.1007/s10495-019-01571-7) contains supplementary material, which is available to authorized users.

✉ Angela Kuhla
angela.kuhla@uni-rostock.de

[1] Institute for Experimental Surgery, Rostock University Medical Center, Schillingallee 69a, 18057 Rostock, Germany

[2] Silence Therapeutics GmbH, Berlin, Germany

APAP-induced liver damage. Until now, it is not clear which form of cell death prevails in APAP toxicity. Accordingly, there are studies, which show that APAP-induced liver cell death is commonly brought upon by necrosis [15, 24–26], however some studies postulate that apoptosis may occur as well [27, 28].

Accordingly, APAP-induced apoptosis is separated in two major pathways, the death receptor-dependent or extrinsic pathway and the mitochondrial-dependent or intrinsic pathway [29–31]. It is characterized by ATP-dependent biochemical mechanisms and apparent morphological changes such as cell shrinking, DNA fragmentation and membrane budding [31]. The apoptotic pathway is linked to the BH3-interacting domain death agonist (Bid), a BH3 only protein, which belongs to the Bcl-2 family and has a pro-apoptotic effect. Bid is commonly activated through death receptor dependent caspase activation, especially caspase-8 [32] or, as a recent study suggested [33], also by other pathomechanisms including mitochondria-related oxidative stress. Truncated Bid, tBid, translocates to the mitochondria. However, at present the molecular events leading to APAP-induced liver injury and failure are not fully understood [15, 26, 34]. It is known that Bid transfers the peripheral apoptotic signals through direct or indirect mechanisms [35–38]. The most noted way to pass on apoptotic signals is the activation of the pro-apoptotic Bcl-2 family members Bak and Bax [39–41], followed by cytochrome c release, which is located in the inner mitochondria membrane. This then deteriorates the respiratory chain and consequently induces oxidative stress. Therefore, mitochondria seem to play an important role in APAP-induced liver damage.

Several studies already showed strategies to inhibit APAP-induced ALF, which however mainly focused on the prevention of APAP-induced liver apoptotic cell death by gene manipulating approaches [28, 42, 43]. For instance, Badmann et al. [43] demonstrated that gene ablation of the pro-apoptotic Bim protein (another Bcl2 family member) substantially protected mice from APAP-induced liver injury [43].

Furthermore, it was shown that liver sinusoidal endothelial cells of Bid knockout mice are significantly protected against APAP toxicity [42]. Also silencing of Bid expression in vitro with short interfering RNA (siRNA) protected liver sinusoidal endothelial cells from cytotoxicity and support the therapeutic hypothesis, that targeting Bid could prevent apoptosis-dependent liver injury [42]. SiRNA therapeutics hold great therapeutic potential, as it is now possible to design and chemically synthesize siRNAs for the safe and efficient targeting of specific genes by RNA interference [44–46]. In addition, targeting gene expression by RNA interference is transient, and can be applied ad hoc in adult mice, thereby reducing the effects of compensatory gene regulation or variable genetic background associated with studies using gene-modified organisms. Therefore, we investigated whether silencing Bid in the liver by short term siRNA application would have hepatoprotective effects in vivo. To inhibit Bid expression in the liver, Bid targeting siRNAs were formulated with a liver-specific siRNA delivery vehicle, DBTC [47] and tested in a murine model for APAP-induced liver injury.

Materials and methods

Animals and in vivo experiments

Male C57BL/6 J mice (Charles River Laboratories, Sulzfeld, Germany) were used at 6–8 weeks of age with a body weight of approximately 20–30 g. Animals were provided water and standard laboratory chow ad libitum. During the night before APAP application, mice were fasted to reduce hepatic glutathione levels. The experimental protocol was approved by the local committee (LALLF 7221.3-1.1-016/14) and all animals received human care according to the German legislation on protection of animals and the Guide for the Care and Use of Laboratory Animals (NIH publication 86–23 revised 1985).

Mice (n = 60) were injected either with in phosphate-buffered saline (PBS) dissolved APAP purchased from SIGMA (99% pure; 300 mg/kg body weight intraperitoneally (bw i.p.) for induction of ALF (n = 30) or with PBS (n = 30) as control and were studied 6 h thereafter (+6 h) as elucidated in Fig. 1a. The animals received 48 h prior to injection of either APAP or PBS a liver-specific small interfering RNA delivery system (DBTC lipoplex), prepared either with Bid siRNA (DBTC/siRNA^{Bid}, n = 20), with non-targeting control siRNA (DBTC/siRNA^{Luci}, n = 20) or with vehicle (vehicle^{HEPES}, n = 20), which served as controls regarding the silencing regimen. For induction of ALF, concentrations of APAP and PBS were used in accordance with work published previously by other groups [34, 48]. The choice to pre-treatment 48 h prior APAP induction is based on the previous study of our group [49]. Since APAP-induced liver cell death was maximally pronounced at +6–12 h [34], we used this time point for the readout of liver damage.

Oligonucleotides

The siRNA molecules used in this study are blunt-ended, double-stranded RNA oligonucleotides (Table 1), stabilized by alternating 2′-*O*-methyl or 2′-F-fluoro modifications,

Table 1 List of siRNA molecules: mA, mU, mC, mG: 2´O-Methyl RNA and fA, fU, fC, fG: 2′deoxy-2′-fluoro RNA

siRNA target	Guide strand	Passenger strand
Bid	5′mUfUmUfGmAfG-mAfUmCfAmGfCmC-mAmUfUmCfGmG 3′	5′fCmCfGmAfAmUfGmGfCmUfGmAfUmCfUmCfAmAfA 3′
Luciferase	5′mUfCmGfAmAfGmU-fAmUfUmCfCmGfC-mGfUmAfCmGfUmG-fAmU 3′	5′fAmUfCmAfCmGfUmAfCmGfCmGfGmAfAmUfAmCfU-mUfCmGfA 3′

Table 2 List of amplicon sets

Target	Amplicon sets	
Bid	mBID:462U20	ACAGCTAGCCGCACAGTTCA
	mBID:552L22	GGCTGTCTTCACCTCATCAAGG
	mBID:493U28FL	CTGTCGGAGGAAGACAAAAGGAACTGCC
Cyp2E1	mCYP2E1:563U22	ATATGCCCTACATGGACGCTGT
	mCYP2E1:652L19	TGTCTCGGGTTGCTTCGTG
	mCYP2E1:603U28L	ATTCATCAACCTCGTCCCTTCCAACCTG
ApoB	mApoB:2889U22	AAAGAGGCCAGTCAAGCTGTTC
	mApoB:2966L22	GGTGGGATCACTTCTGTTTTGG
	mApoB:2916U29FL	CAGCAACACACTGCATCTGGTCTCTACCA

respectively, on both strands as previously described [50, 51] and were synthesized by Biospring (Frankfurt a.M., Germany). For in vivo application, siRNAs were formulated with DBTC, a liver specific siRNA delivery system developed by Silence Therapeutics GmbH for targeting specifically the liver [47].

Intravital fluorescence microscopy

For in vivo analysis of hepatocellular apoptosis, intrahepatic leukocyte accumulation and sinusoidal perfusion failure, fluorescence microscopy was performed 6 h after APAP exposure in ketamine/xylazine-anesthetized animals (75/25 mg/kg [bw, ip]) in accordance with work previously published by our group [52, 53]. Further details are provided in supplemental materials and methods.

Sampling and assays

After in vivo microscopy, animals were exsanguinated by puncture of the vena cava inferior for immediate separation of EDTA plasma. The degree of hepatic disintegration was assessed by spectrophotometric determination of plasma alanine aminotransferase (ALT) and aspartate aminotransferase (AST) activities using commercially available reaction kits (Roche Diagnostics, Mannheim, Germany). Cyclophilin A (indicator for necrotic cell death) and HMGB1 (indicator for necrotic cell death and sterile inflammation) were measured using ELISA Kits according to the manufacturer´s instructions (HMGB1: IBL International GmbH, Hamburg, Germany and cyclophilin A: LSBio, LifeSpab BioScience, Inc., Seattle, WA). Liver tissue was sampled for Western blot, real time-PCR as well as hepatic GSH analysis and histology.

Real time-PCR (RT-PCR) analysis

Approximately 20 mg of tissue was homogenized in a Mixer Mill MM 301 (Retsch GmbH, Haan, Germany) using tungsten carbide beads (Qiagen). Total RNA was isolated via the Invisorb Spin Tissue RNA Mini Kit (Invitek, Berlin, Germany). Depending on the tissue, 25–100 ng total RNA was used for quantitative TaqMan Real Time (RT)-PCR with the amplicon set]s (for Bid, cytochrome P450 2E1 (cyp2E1), ApoB, see Table 2) obtained from BioTez GmbH, Berlin, Germany: The TaqMan RT-PCR reactions were carried out with an ABI PRISM 7700 Sequence Detector (Software: Sequence Detection System v1.6.3 (ABI)) or StepOnePlus™ RT-PCR Sytem (ABI) using a standard protocol for RT-PCR as described previously [50] and probes at a concentration of 300 and 100 nM respectively. TaqMan data were calculated by using the comparative CT method.

Western blot analysis

Target protein expression was assessed by Western blotting of whole tissue lysates. Snap frozen tissues were homogenized in lysis buffer (10 mM Tris pH 7.5, 10 mM NaCl,

0.1 mM EDTA, 0.5% Triton-X 100, 0.02% NaN3), and 0.2 mM PMSF (a protease inhibitor cocktail), incubated for 30 min on ice and centrifuged for 10 min at 4 °C and 10,000×*g*. Protein contents were assayed by the bicinchoninic acid method (Pierce Biotechnology) with 2.5% BSA (Pierce Biotechnology) as standard. On 14% SDS gels, 40 µg protein from liver tissue was separated and transferred to a polyvinyldifluoride membrane (Immobilon-P; Millipore). After blockade with 2.5% BSA (Pierce Biotechnology), membranes were incubated overnight at 4 °C with following antibodies: a mouse monoclonal anti-Bax (1:250, BD Pharmingen, Heidelberg, Germany), a mouse monoclonal anti-bcl2 (1:500, BD Pharmingen), a mouse monoclonal anti-Bid (1:1000, Santa Cruz Biotechnology, Texas, USA) and a mouse monoclonal anti-ß-actin (1:20,000; Sigma-Aldrich, Taufkirchen, Germany) or rabbit alpha-actinin antibody (1:500, Cell Signaling, Frankfurt) for loading control. Afterwards, secondary peroxidase-linked anti-mouse antibodies (Bax and Bcl2; 1:20,000; ß-actin; 1:60,000) or anti-rabbit antibodies (1:40,000) were applied. Protein expression was visualized by means of luminol-enhanced chemiluminescence (ECL plus; Amersham Pharmacia Biotech) and digitalized with ChemiDoc™ XRS System (Bio-Rad Laboratories). Signals were densitometrically assessed (Quantity One; Bio-Rad Laboratories) and normalized to ß-actin. Bid and alpha-actinin blots were analysed using Stella camera system and AIDA image analyser software 4.25 from Raytest (Mannheim, Germany).

Hepatic glutathione (GSH) analysis

For measurement of hepatic GSH content, livers were homogenized with 50 mM phosphate puffer containing 1 mM EDTA (pH 6-7) and deproteinized with metaphosphoric acid and triethanolamine. The GSH content was analysed by using the glutathione assay kit method according to the manufacturer's instructions (Cayman Chemical Company, MI, USA) and is given as µmol/g liver tissue.

Histology

Liver tissue was fixed in 4% phosphate-buffered formalin for 2–3 days and then embedded in paraffin. 4 µm sections were fixed on glass slides and stained with haematoxylin and eosin (H & E). For histomorphometric analysis of necrotic tissue images of twenty random low-power fields (×10 magnification, Olympus BX 51, Hamburg, Germany) were acquired with a Colour View II FW camera (Colour View, Munich, Germany). The quotient of the focal necrosis surface to the total liver section area was assessed and given in percent.

Statistical analysis

All data are expressed as means + SEM. For statistics, one-way analysis of variance, including all groups, was used to assess significant differences between groups. Subsequently, post hoc pairwise comparison test including Bonferroni correction for multiple comparisons was applied to identify which group differs to each other. Data were considered significant if $p < 0.05$. Statistical analysis was performed using the SigmaStat software package (Jandel Corporation, San Rafael, CA, USA). The results were presented with the program SigmaPlot 11.0 (Jandel Corporation, San Rafael, CA, USA).

Results

Effects of Bid silencing in mice treated with APAP

In order to evaluate whether hepatic silencing of Bid was effective, Bid mRNA and protein levels were assessed in liver samples collected 54 h after mice were treated with DBTC/siRNA^{Bid} formulation by i.v. administration (Fig. 1b, c). At this time point, Bid mRNA levels were significantly decreased compared to the control groups treated with the vehicle^{HEPES} or with non-targeting control lipoplex, DBTC/siRNA^{Luci} (Fig. 1b). Similarly, hepatic Bid protein levels were markedly decreased in siRNA^{Bid}-versus vehicle^{HEPES}-treated mice as shown by a representative Western blot (Fig. 1c). The quantitative densitometric analysis revealed an about 70% reduction of Bid protein levels (siRNA^{Bid} vs. vehicle^{Hepes} $n = 8$ each, $p = 0.013$, data not shown). Furthermore, siRNA^{Bid} treatment attenuated the APAP-induced upregulation of Bax protein expression, as shown by an only twofold rise of Bax protein expression versus a three to fourfold rise in siRNA^{Luci} and vehicle^{HEPES} pre-treated mice (Fig. 2a, $p < 0.05$ vs. siRNA^{Luci}). Bcl2 protein expression was only slightly increased in livers of siRNA^{Bid} pre-treated mice while APAP caused a 1.5-to twofold rise in siRNA^{Luci} and vehicle^{HEPES} pre-treated mice (Fig. 2b). To evaluate whether Bid silencing before APAP exposure has the potential for off-target effects, we investigated hepatic *cyp2E1* mRNA expression and hepatic GSH content. APAP exposure led to a reduction of relative *cyp2E1* mRNA expression in all three groups with comparable values

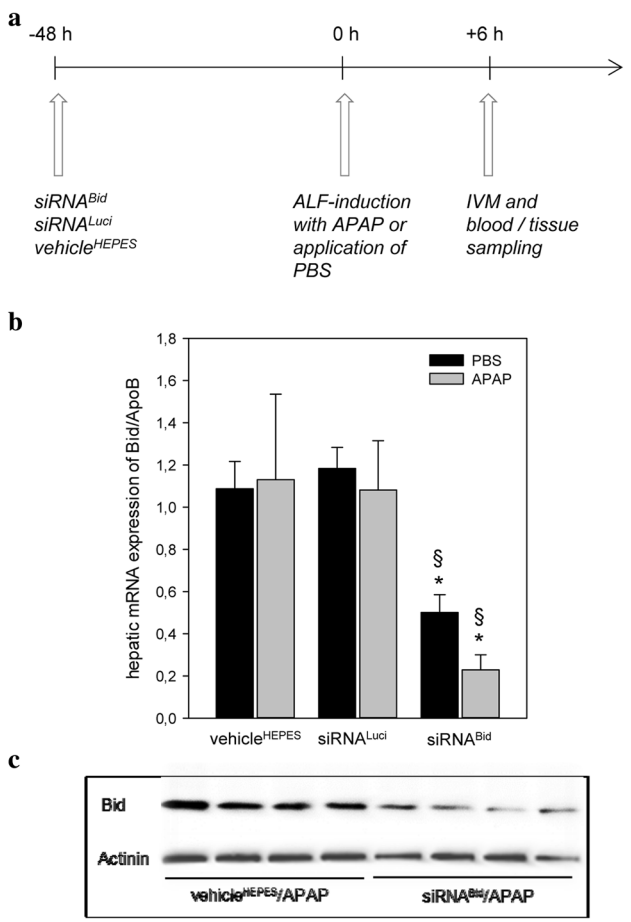

Fig. 1 **a** Schematic illustration of the experimental design and **b** quantitative RT-PCR analysis of Bid mRNA expression in livers of treated C57BL/6 J mice (n = 60). All animals received 42 h prior to injection of either APAP (n = 30) or PBS (n = 30, 300 mg/kg body weight per mice intraperitoneally (bw i.p.)) a liver-specific small interfering RNA delivery system (DBTC/siRNA^{Bid} (n = 20) or DBTC/siRNA^{Luci} (n = 20) or DBTC/vehicle^{HEPES} (n = 20)). For the control group we did the same pre-treatment but with equivalent volumes of phosphate-buffered saline (PBS) instead of APAP. Mice were studied 6 h thereafter (+6 h). **c** Representative western blot of the hepatic Bid protein expression with loading control of actinin in livers of DBTC/vehicle^{HEPES} + APAP-(n = 4) and DBTC/siRNA^{Luci} + APAP-(n = 4) treated mice. Signals were corrected to that of ApoB. Values are given as mean + SEM; ANOVA, post hoc pairwise comparison tests, Bonferroni correction: *p < 0.05 versus DBTC/siRNA^{Luci}; §p < 0.05 versus DBTC/vehicle^{HEPES}

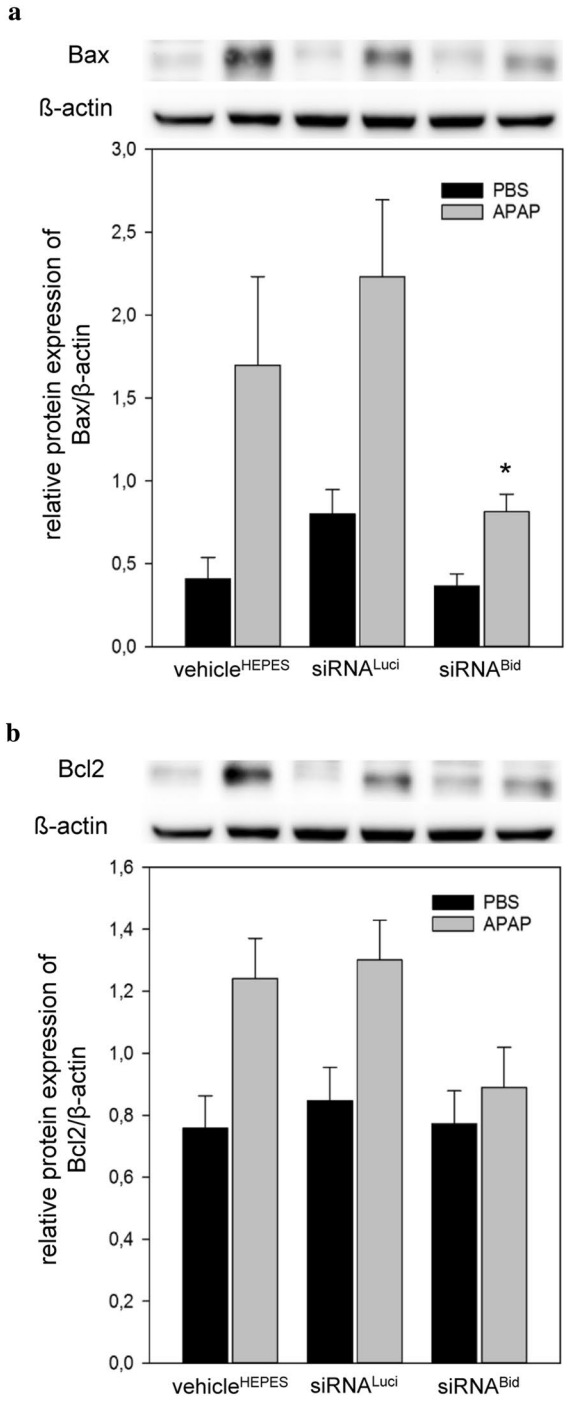

Fig. 2 Representative western blot images (upper panels) and quantitative analysis of hepatic protein expression of **a** Bax and **b** Bcl2 in livers of treated C57BL/6 J mice (n = 60). Signals were corrected to that of ß-actin. All animals received 42 h prior to injection of either APAP (n = 30) or PBS (n = 30, 300 mg/kg body weight per mice intraperitoneally (bw i.p.)) a liver-specific small interfering RNA delivery system (DBTC/siRNA^{Bid} (n = 20) or DBTC/siRNA^{Luci} (n = 20) or DBTC/vehicle^{HEPES} (n = 20)). For the control group we did the same pre-treatment but with equivalent volumes of phosphate-buffered saline (PBS) instead of APAP. Mice were studied 6 h thereafter (+6 h). Values are given as mean + SEM; ANOVA, post hoc pairwise comparison tests, Bonferroni correction: *p < 0.05 versus DBTC/siRNA^{Luci}

in vehicle^{HEPES}/APAP-(0.80 ± 0.07), siRNA^{Luci}/APAP-(0.85 ± 0.07; p = 0.007) and siRNA^{Bid}/APAP-(0.78 ± 0.07) exposed mice when compared to PBS-exposed mice (relative *cyp2E1* mRNA expression 1.15 ± 0.09 at average). Similarly, the content of hepatic GSH with 6.6 ± 0.1 µmol/g liver tissue in the siRNA^{Bid}/APAP group was almost unchanged when compared to values of the vehicle^{HEPES}/APAP (6.3 ± 0.05 µmol/g) or siRNA^{Luci}/APAP (6.5 ± 0.06 µmol/g) groups.

Bid silencing decreased APAP-induced necrotic cell death and sterile inflammation

Hepatocellular DNA fragmentation was almost absent in livers of PBS-treated mice, while APAP caused a dramatic rise in cell death, evident by the high number (200–300 hepatocytes/mm^2) with DNA fragmentation in siRNA^{Luci} and vehicle^{HEPES} pre-treated control mice (Fig. 3a, right panel, $p < 0.05$ vs. PBS). Administration of siRNA^{Bid} significantly reduced the APAP-associated cell death to only approx. 70 cells/mm^2 (Fig. 3a, $p < 0.05$ vs. PBS, siRNA^{Luci} and vehicle^{HEPES}). The reduction of cell death by Bid silencing let to a general reduction of typical signs of liver damage. This is illustrated by a significant reduction of necrotic tissue in liver sections (Fig. 3b, $p < 0.05$ vs. PBS, siRNA^{Luci} and vehicle^{HEPES}) and a decrease in the plasma levels of the transaminases ALT and AST when

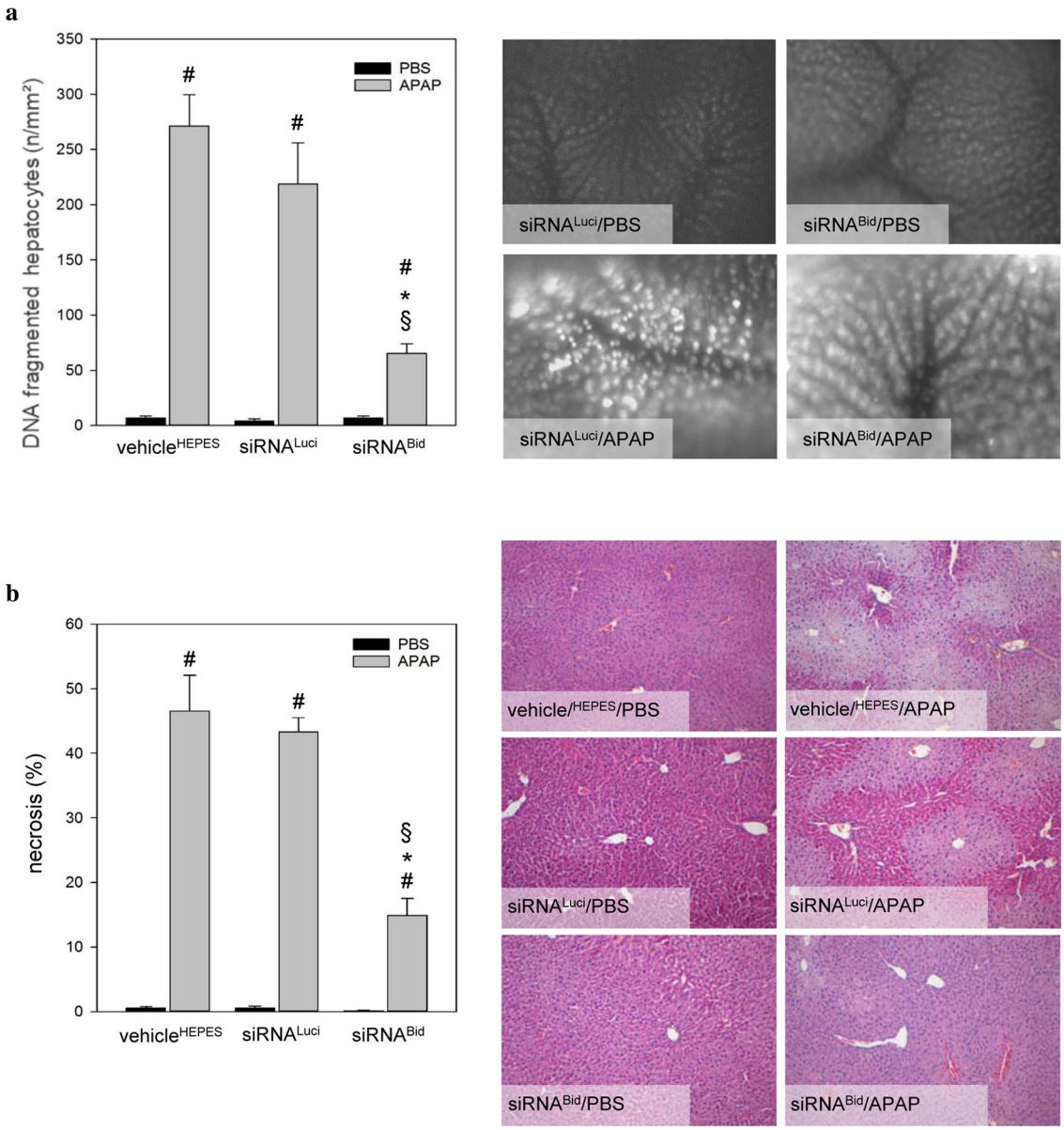

Fig. 3 Quantitative analysis of **a** DNA fragmented hepatocytes as well as representative images of intravital fluorescence microscopy (right panel; original magnification ×200) and of **b** necrotic tissue area (in %) as well as representative H&E stained liver specimen (right panel; original magnification ×100). C57BL/6 J mice (n = 60) received 42 h prior to injection of either APAP (n = 30) or PBS (n = 30, 300 mg/kg body weight per mice intraperitoneally (bw i.p.)) a liver-specific small interfering RNA delivery system (DBTC/siRNA^{Bid} (n = 20) or DBTC/siRNA^{Luci} (n = 20) or DBTC/vehicle^{HEPES} (n = 20)). For the control group we did the same pre-treatment but with equivalent volumes of phosphate-buffered saline (PBS) instead of APAP. Mice were studied 6 h thereafter (+6 h). Values are given as mean + SEM; ANOVA, post hoc pairwise comparison tests, Bonferroni correction: $^{\#}p < 0.05$ vs. PBS; $^{*}p < 0.05$ versus DBTC/siRNA^{Luci}; $^{\S}p < 0.05$ versus DBTC/vehicle^{HEPES}

compared to mice treated with control siRNAs (Fig. 4a, b). The plasma concentration of HMGB1, a strong indicator of necrotic cell death and sterile inflammation, was also significantly reduced in siRNA^{Bid}-treated APAP-exposed mice (Fig. 4c, $p < 0.05$ vs. siRNA^{Luci}). Furthermore, the concentration of cyclophilin A tended to be lowest in siRNA^{Bid}-treated mice (Fig. 4d).

Bid silencing did not affect APAP-induced non-sterile inflammation and sinusoidal perfusion failure

In vivo microscopy of livers of APAP-exposed mice revealed characteristic features of acute non-sterile inflammation (Fig. 5a–c) with markedly increased numbers of both rolling and adherent leukocytes in postsinusoidal venules (Fig. 5a, b, $p < 0.05$ vs. PBS) as well as of tissue-infiltrating

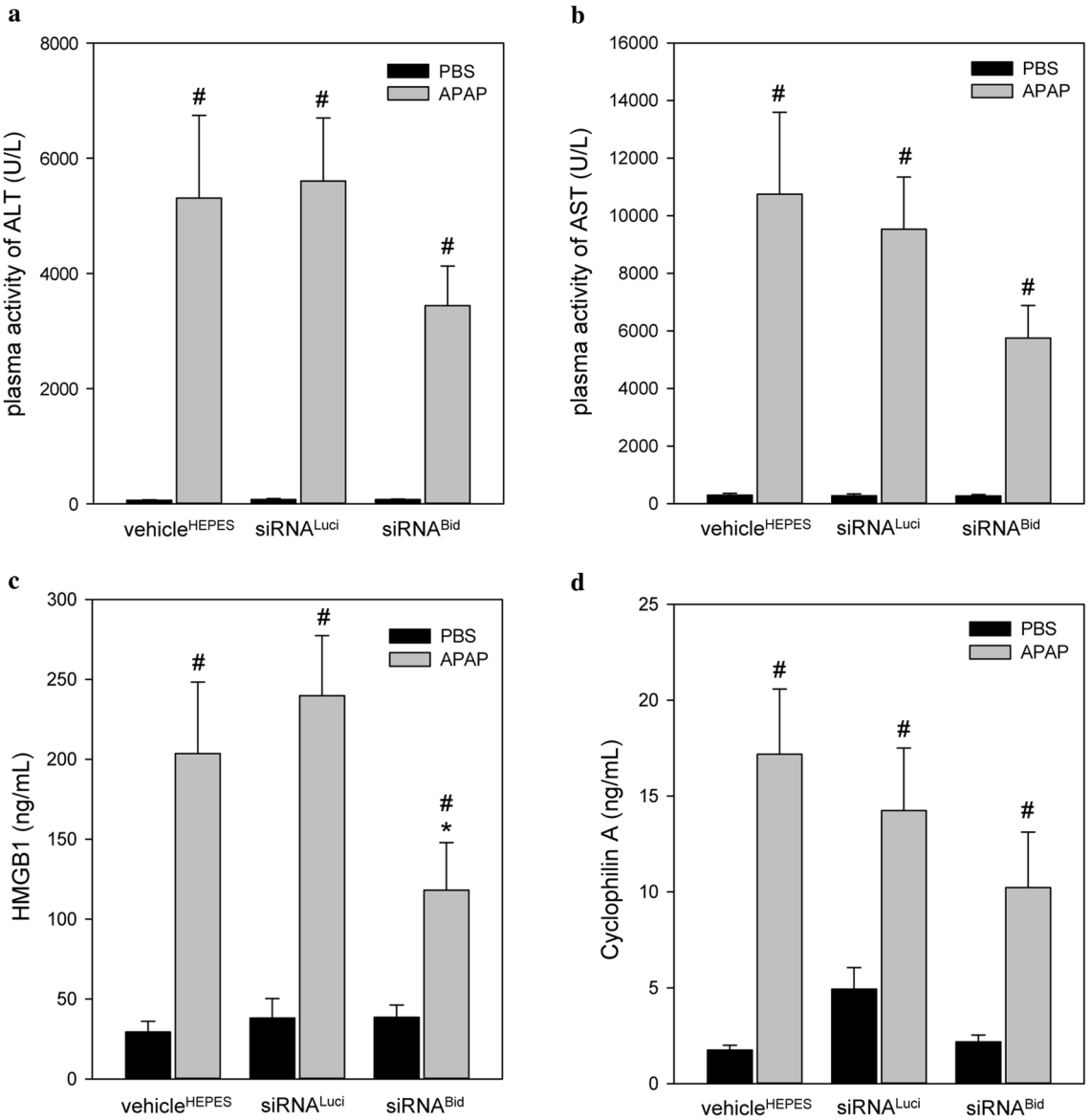

Fig. 4 Plasma activities of **a** alanine aminotransferase (ALT) and **b** aspartate aminotransferase (AST) as well as plasma concentrations of **c** HMGB1 and of **d** cyclophilin A. C57BL/6 J mice (n = 60) received 42 h prior to injection of either APAP (n = 30) or PBS (n = 30, 300 mg/kg body weight per mice intraperitoneally (bw i.p.)) a liver-specific small interfering RNA delivery system (DBTC/siRNA^{Bid} (n = 20) or DBTC/siRNA^{Luci} (n = 20) or DBTC/vehicle^{HEPES} (n = 20)). For the control group we did the same pre-treatment but with equivalent volumes of phosphate-buffered saline (PBS) instead of APAP. Mice were studied 6 h thereafter (+6 h). Values are given as mean + SEM; ANOVA, post hoc pairwise comparison tests, Bonferroni correction: $^{\#}p < 0.05$ versus PBS; $^{*}p < 0.05$ versus DBTC/siRNA^{Luci}

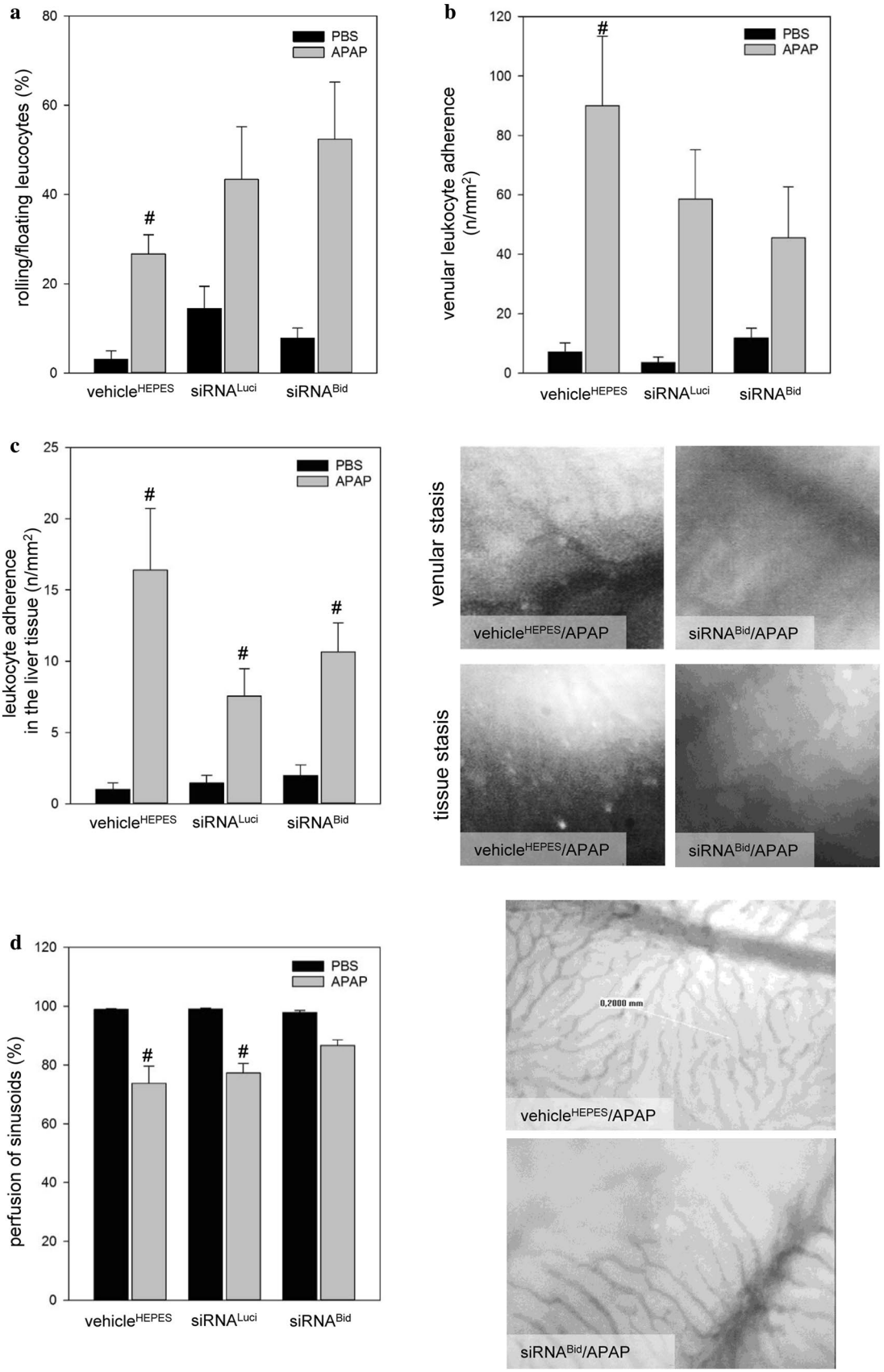
a
rolling/floating leucocytes (%)
PBS
APAP
vehicle^HEPES
siRNA^Luci
siRNA^Bid
b
venular leukocyte adherence (n/mm²)
c
leukocyte adherence in the liver tissue (n/mm²)
venular stasis
tissue stasis
vehicle^HEPES/APAP
siRNA^Bid/APAP
d
perfusion of sinusoids (%)
0,2000 mm

◂**Fig. 5** Quantitative analysis of **a** rolling vs. floating leukocytes, **b** adherent leukocytes in postsinusoidal venules as well as **c** of tissue infiltrating leukocytes with representative images of intravital fluorescence microscopy (+6 h) (right middle panel, original magnification ×200). Quantitative analysis of **d** sinusoidal perfusion with representative images of intravital fluorescence microscopy (right lower panel, original magnification ×200). C57BL/6 J mice (n = 60) received 42 h prior to injection of either APAP (n = 30) or PBS (n = 30, 300 mg/kg body weight per mice intraperitoneally (bw i.p.)) a liver-specific small interfering RNA delivery system (DBTC/siRNA^{Bid} (n = 20) or DBTC/siRNA^{Luci} (n = 20) or DBTC/vehicle^{HEPES} (n = 20)). For the control group we did the same pre-treatment but with equivalent volumes of phosphate-buffered saline (PBS) instead of APAP. Mice were studied 6 h thereafter (+6 h). Values are given as mean + SEM; ANOVA, post hoc pairwise comparison tests, Bonferroni correction: $^{\#}p < 0.05$ versus PBS

leukocytes (Fig. 5c, $p < 0.05$ vs. PBS) when compared to PBS-treated mice. APAP-induced non-sterile inflammation as assessed by intrahepatic leukocyte flow behaviour did not significantly differ between the different siRNA treated groups (Fig. 5a–c).

Next to non-sterile inflammation, livers of APAP-exposed mice revealed a marked sinusoidal perfusion failure. Of interest, perfusion deficit was highest in vehicle^{HEPES} and siRNA^{Luci} pre-treated mice with approx. 32% non-perfused (Fig. 5d, right panel, $p < 0.05$ vs. PBS) sinusoids, while siRNA^{Bid} pre-treated mice showed ~ 20% less perfusion failure (Fig. 5d, right panel).

Discussion

The worldwide leading cause of acute liver failure (ALF) is intoxication by APAP. However, the pathogenesis of hepatic injury under APAP treatment is still not completely clarified [15, 22]. On the one hand side, recent studies [34, 54, 55] discovered that non-sterile inflammation represented by infiltration of inflammatory cells occurs in APAP-induced liver damage, but is not the main contributor of ALF [22, 34, 54, 55]. On the other hand, many studies described that APAP-induced liver pathology is characterized by sterile inflammation wherein the innate immune response is activated by pathogenic-derived molecules such as HMGB1 [56, 57]. The present study confirms now that both non-sterile and sterile inflammation upon APAP exposure occurs as indicated by intrahepatic leukocyte accumulation as well as raised HMGB1 plasma concentrations.

Beside inflammation, the microcirculation is deteriorated in APAP-induced liver failure [58]. Likewise, hepatic sinusoids of APAP-exposed livers showed failure of perfusion. This may directly trigger cytotoxic effector mechanisms [42, 58] contributing to apoptotic and necrotic cell death. Until today, there is ongoing discussion on the predominant form of cell death in APAP-induced ALF with reports on apoptosis, necrosis, necroptosis and regulated necrosis [22, 59–61]. Latest research discovered DNA-fragmented cells during cell death in regulated necrosis [25, 31, 62], a feature that was originally assigned to apoptosis [27, 28, 33, 63]. In the present study we used bisbenzimide for in vivo staining of hepatic tissue, which showed DNA fragmentation and condensation, most probably depicting cells undergoing apoptosis [27, 28]. At the same time, significant increases of plasma AST and ALT activities and the presence of large and confluent areas of necrotic tissue in APAP-treated mice indicate that also necrosis occurs as an additional pathway upon APAP intoxication. In this context, it has to be mentioned that male mice -as used in the present study- are particular susceptible to APAP-induced ALF and showing significantly higher increases of plasma AST and ALT activities than female mice [64]. Besides transaminase, plasma concentrations of HMGB1 and cyclophilin A were significantly increased upon APAP exposure. Necrosis as the predominant part of APAP-induced ALF was further affirmed by failure of caspase-3 activation (data not shown) which was already shown by many other studies [28, 60, 62, 65]. In case of ATP deficiency cells shift from apoptosis to necrosis [33, 66]. Upon APAP-treatment mitochondrial proteins are especially affected [12, 16–18], leading to impaired respiratory chain, oxidative stress and in consequence to lack of ATP. Thus, cell showing DNA fragmentation will further undergo necrotic cell death.

In regulated necrosis newest studies described pathway upon APAP treatment, such as translocation of the BH3-interacting domain death agonist (Bid) and Bcl-2-associated X protein (Bax), which were first attributed to apoptosis but are now becoming even more important in necrosis [33, 67–69]. Thus, the marked increase of Bax protein suggests that APAP-induced ALF is mainly characterized by necrotic signals.

In previous in vivo studies using Bid knockout mice [42] and in vitro studies employing Bid silencing [42] it was proposed that inhibition of the Bid pathway has therapeutic potential to reduce ALF. Although the present study does not represent a therapeutic approach, we confirmed and extent the current literature by showing that transient liver-specific targeting of Bid expression using liposomal siRNA delivery has hepatoprotective effects. This formulation was already used in a previous study silencing Fas expression 48 h prior to induction of ALF [49] and showing a protection against apoptotic and necrotic cell death as well as microcirculatory dysfunction. Several lipid nanoparticles for oligonucleotide delivery are currently in preclinical and clinical development [70, 71] and the first siRNA lipid nanoparticle has been approved by the US Food and Drug administration in August 2018 [72]. In addition, N-acetylgalactosamine (GalNAc) siRNA conjugates for liver targeting hold great promise for safe and efficacious therapeutic compounds with the ease of subcutaneous

administration and with many GalNAc siRNA conjugates in clinical development [72–74]. In the present study, an about 70% reduction of Bid protein expression was sufficient to ameliorate liver injury, indicating that Bid could be a sensible target for siRNA-based therapeutics or other targeting approaches. The failure of $siRNA^{Bid}$ to influence hepatic *cyp2E1* expression and GSH content implies that this strategy lacks off-target effects and seems to be specific.

We could demonstrate that the number of bisbenzimide-stained DNA-fragmented hepatocytes were markedly reduced upon Bid silencing, supporting Bid as a major player in APAP-induced necrotic liver tissue damage. Since Bax-silenced mice were protected from APAP-induced ALF [48], reduced Bax protein expression upon Bid silencing might also contribute to the attenuated liver damage. The fact that mitochondrial translocations of tBid and Bax are closely related and have similar effects on the molecular pathomechanism of necrosis [33, 67, 68], it is reasonable to assume that necrosis rather than apoptosis triggered APAP-induced liver tissue damage. This view is further supported by the reduction of necrotic tissue area, HMGB1 concentrations, as well as plasma activities of AST and ALT. Thus, necrosis might be the predominant cell death pathway as reported by many other studies observing a form of regulated necrosis upon APAP intoxication [22, 59–61, 75].

In summary, Bid silencing mediated tissue protection against APAP most probably via reduced (i) expression of Bid and Bax, (ii) execution of necrotic cell death and (iii) release of HMGB1 as a marker of sterile inflammation.

Acknowledgments The authors cordially thank Berit Blendow, Dorothea Frenz, Maren Nerowski, and Eva Lorbeer (Institute for Experimental Surgery, University of Rostock, Germany) for excellent technical assistance.

Compliance with ethical standards

Conflict of interest Ute Schaeper and Sibylle Dames are employees of Silence Therapeutics GmbH and declare competing financial interest. The other authors declare that they have no conflict of interest.

References

1. Lee WM, Squires RH, Nyberg SL et al (2008) Acute liver failure: summary of a workshop. Hepatology 47(4):1401–1415
2. Bernal W, Wendon J (2013) Acute liver failure. N Engl J Med 369:2525–2534. https://doi.org/10.1056/NEJMra1208937
3. Gow PJ, Jones RM, Dobson JL, Angus PW (2004) Etiology and outcome of fulminant hepatic failure managed at an Australian liver transplant unit. J Gastroenterol Hepatol 19:154–159
4. Reuben A, Koch DG, Lee WM (2010) Drug-induced acute liver failure: results of a U.S. multicenter, prospective study. Hepatology 52:2065–2076. https://doi.org/10.1002/hep.23937
5. Larson AM, Polson J, Fontana RJ et al (2005) Acetaminophen-induced acute liver failure: results of a United States multicenter, prospective study. Hepatology 42:1364–1372. https://doi.org/10.1002/hep.20948
6. Fontana RJ (2008) Acute liver failure including acetaminophen overdose. Med Clin North Am 92:761–794. https://doi.org/10.1016/j.mcna.2008.03.005
7. Lee WM (2004) Acetaminophen and the U.S. acute liver failure study group: lowering the risks of hepatic failure. Hepatology 40:6–9. https://doi.org/10.1002/hep.20293
8. Lancaster EM, Hiatt JR, Zarrinpar A (2015) Acetaminophen hepatotoxicity: an updated review. Arch Toxicol 89:193–199. https://doi.org/10.1007/s00204-014-1432-2
9. Jaeschke H, Knight TR, Bajt ML (2003) The role of oxidant stress and reactive nitrogen species in acetaminophen hepatotoxicity. Toxicol Lett 144:279–288
10. Jaeschke H, Bajt ML (2006) Intracellular signaling mechanisms of acetaminophen-induced liver cell death. Toxicol Sci 89:31–41. https://doi.org/10.1093/toxsci/kfi336
11. Yan H-M, Ramachandran A, Bajt ML et al (2010) The oxygen tension modulates acetaminophen-induced mitochondrial oxidant stress and cell injury in cultured hepatocytes. Toxicol Sci 117:515–523. https://doi.org/10.1093/toxsci/kfq208
12. Nelson SD (1990) Molecular mechanisms of the hepatotoxicity caused by acetaminophen. Semin Liver Dis 10:267–278. https://doi.org/10.1055/s-2008-1040482
13. Adams ML, Pierce RH, Vail ME et al (2001) Enhanced acetaminophen hepatotoxicity in transgenic mice overexpressing BCL-2. Mol Pharmacol 60:907–915
14. Reid AB, Kurten RC, McCullough SS et al (2005) Mechanisms of acetaminophen-induced hepatotoxicity: role of oxidative stress and mitochondrial permeability transition in freshly isolated mouse hepatocytes. J Pharmacol Exp Ther 312:509–516. https://doi.org/10.1124/jpet.104.075945
15. Jaeschke H, McGill MR, Ramachandran A (2012) Oxidant stress, mitochondria, and cell death mechanisms in drug-induced liver injury: lessons learned from acetaminophen hepatotoxicity. Drug Metab Rev 44:88–106. https://doi.org/10.3109/03602532.2011.602688
16. Cohen SD, Khairallah EA (1997) Selective protein arylation and acetaminophen-induced hepatotoxicity. Drug Metab Rev 29:59–77
17. Jaeschke H, Williams CD, McGill MR et al (2013) Models of drug-induced liver injury for evaluation of phytotherapeutics and other natural products. Food Chem Toxicol 55:279–289. https://doi.org/10.1016/j.fct.2012.12.063
18. McGill MR, Lebofsky M, Norris H-RK et al (2013) Plasma and liver acetaminophen-protein adduct levels in mice after acetaminophen treatment: dose-response, mechanisms, and clinical implications. Toxicol Appl Pharmacol 269:240–249. https://doi.org/10.1016/j.taap.2013.03.026
19. Hu J, Ramshesh VK, McGill MR et al (2016) Low dose acetaminophen induces reversible mitochondrial dysfunction associated with transient c-Jun N-terminal kinase activation in mouse liver. Toxicol Sci 150:204–215. https://doi.org/10.1093/toxsci/kfv319
20. Jaeschke H (2015) Acetaminophen: dose-dependent drug hepatotoxicity and acute liver failure in patients. Dig Dis 33:464–471. https://doi.org/10.1159/000374090
21. Tirmenstein MA, Nelson SD (1989) Subcellular binding and effects on calcium homeostasis produced by acetaminophen and a nonhepatotoxic regioisomer, 3'-hydroxyacetanilide, in mouse liver. J Biol Chem 264:9814–9819
22. Ramachandran A, Jaeschke H (2018) Acetaminophen toxicity: novel insights into mechanisms and future perspectives. Gene Expr 18:19–30. https://doi.org/10.3727/105221617X15084371374138
23. Kubes P, Mehal WZ (2012) Sterile inflammation in the liver. Gastroenterology 143:1158–1172. https://doi.org/10.1053/j.gastro.2012.09.008

24. Burcham PC, Harman AW (1991) Acetaminophen toxicity results in site-specific mitochondrial damage in isolated mouse hepatocytes. J Biol Chem 266:5049–5054
25. Cover C, Mansouri A, Knight TR et al (2005) Peroxynitrite-induced mitochondrial and endonuclease-mediated nuclear DNA damage in acetaminophen hepatotoxicity. J Pharmacol Exp Ther 315:879–887. https://doi.org/10.1124/jpet.105.088898
26. Jaeschke H, Williams CD, Farhood A (2011) No evidence for caspase-dependent apoptosis in acetaminophen hepatotoxicity. Hepatology 53:718–719. https://doi.org/10.1002/hep.23940
27. Ray SD, Jena N (2000) A hepatotoxic dose of acetaminophen modulates expression of BCL-2, BCL-X(L), and BCL-X(S) during apoptotic and necrotic death of mouse liver cells in vivo. Arch Toxicol 73:594–606
28. El-Hassan H, Anwar K, Macanas-Pirard P et al (2003) Involvement of mitochondria in acetaminophen-induced apoptosis and hepatic injury: roles of cytochrome c, Bax, Bid, and caspases. Toxicol Appl Pharmacol 191:118–129
29. Kon K, Ikejima K, Okumura K et al (2007) Role of apoptosis in acetaminophen hepatotoxicity. J Gastroenterol Hepatol 22(Suppl 1):S49–S52. https://doi.org/10.1111/j.1440-1746.2007.04962.x
30. Zimmermann KC, Bonzon C, Green DR (2001) The machinery of programmed cell death. Pharmacol Ther 92:57–70
31. Elmore S (2007) Apoptosis: a review of programmed cell death. Toxicol Pathol 35:495–516. https://doi.org/10.1080/01926230701320337
32. Esposti MD (2002) The roles of Bid. Apoptosis 7:433–440
33. Karch J, Molkentin JD (2015) Regulated necrotic cell death: the passive aggressive side of Bax and Bak. Circ Res 116:1800–1809. https://doi.org/10.1161/CIRCRESAHA.116.305421
34. Jaeschke H, McGill MR, Williams CD, Ramachandran A (2011) Current issues with acetaminophen hepatotoxicity—a clinically relevant model to test the efficacy of natural products. Life Sci 88:737–745. https://doi.org/10.1016/j.lfs.2011.01.025
35. Willis SN, Adams JM (2005) Life in the balance: how BH3-only proteins induce apoptosis. Curr Opin Cell Biol 17:617–625. https://doi.org/10.1016/j.ceb.2005.10.001
36. Lutter M, Fang M, Luo X et al (2000) Cardiolipin provides specificity for targeting of tBid to mitochondria. Nat Cell Biol 2:754–761. https://doi.org/10.1038/35036395
37. Scorrano L, Ashiya M, Buttle K et al (2002) A distinct pathway remodels mitochondrial cristae and mobilizes cytochrome c during apoptosis. Dev Cell 2:55–67
38. Soriano ME, Scorrano L (2011) Traveling Bax and forth from mitochondria to control apoptosis. Cell 145:15–17. https://doi.org/10.1016/j.cell.2011.03.025
39. Wei MC, Zong WX, Cheng EH et al (2001) Proapoptotic BAX and BAK: a requisite gateway to mitochondrial dysfunction and death. Science 292:727–730. https://doi.org/10.1126/science.1059108
40. Cartron P-F, Gallenne T, Bougras G et al (2004) The first alpha helix of Bax plays a necessary role in its ligand-induced activation by the BH3-only proteins Bid and PUMA. Mol Cell 16:807–818. https://doi.org/10.1016/j.molcel.2004.10.028
41. Kim H, Rafiuddin-Shah M, Tu H-C et al (2006) Hierarchical regulation of mitochondrion-dependent apoptosis by BCL-2 subfamilies. Nat Cell Biol 8:1348–1358. https://doi.org/10.1038/ncb1499
42. Badmann A, Langsch S, Keogh A et al (2012) TRAIL enhances paracetamol-induced liver sinusoidal endothelial cell death in a Bim- and Bid-dependent manner. Cell Death Dis 3:e447. https://doi.org/10.1038/cddis.2012.185
43. Badmann A, Keough A, Kaufmann T et al (2011) Role of TRAIL and the pro-apoptotic Bcl-2 homolog Bim in acetaminophen-induced liver damage. Cell Death Dis 2:e171–e171. https://doi.org/10.1038/cddis.2011.55
44. Farra R, Pozzato G, Dapas B et al (2006) 251 A sirna targeted against srf reduces hepatocellular carcinoma cell proliferation, showing its potential use in the growth inhibition of this type of tumour. J Hepatol 44:S100. https://doi.org/10.1016/S0168-8278(06)80252-7
45. Dapas B, Farra R, Grassi M et al (2009) Role of E2F1-cyclin E1-cyclin E2 circuit in human coronary smooth muscle cell proliferation and therapeutic potential of its downregulation by siRNAs. Mol Med 15:297–306. https://doi.org/10.2119/molmed.2009.00030
46. Farra R, Dapas B, Pozzato G et al (2010) Serum response factor depletion affects the proliferation of the hepatocellular carcinoma cells HepG2 and JHH6. Biochimie 92:455–463. https://doi.org/10.1016/j.biochi.2010.01.007
47. Abshagen K, Brensel M, Genz B et al (2015) Foxf1 siRNA delivery to hepatic stellate cells by DBTC lipoplex formulations ameliorates fibrosis in livers of bile duct ligated mice. Curr Gene Ther 15:215–227
48. Bajt ML, Farhood A, Lemasters JJ, Jaeschke H (2008) Mitochondrial bax translocation accelerates DNA fragmentation and cell necrosis in a murine model of acetaminophen hepatotoxicity. J Pharmacol Exp Ther 324:8–14. https://doi.org/10.1124/jpet.107.129445
49. Kuhla A, Thrum M, Schaeper U et al (2015) Liver-specific Fas silencing prevents galactosamine/lipopolysaccharide-induced liver injury. Apoptosis 20:500–511. https://doi.org/10.1007/s10495-015-1088-2
50. Santel A, Aleku M, Keil O et al (2006) RNA interference in the mouse vascular endothelium by systemic administration of siRNA-lipoplexes for cancer therapy. Gene Ther 13:1360–1370. https://doi.org/10.1038/sj.gt.3302778
51. Czauderna F, Fechtner M, Dames S et al (2003) Structural variations and stabilising modifications of synthetic siRNAs in mammalian cells. Nucleic Acids Res 31:2705–2716
52. Eipel C, Kidess E, Abshagen K et al (2007) Antileukoproteinase protects against hepatic inflammation, but not apoptosis in the response of D-galactosamine-sensitized mice to lipopolysaccharide. Br J Pharmacol 151:406–413. https://doi.org/10.1038/sj.bjp.0707230
53. Le Minh K, Klemm K, Abshagen K et al (2007) Attenuation of inflammation and apoptosis by pre- and posttreatment of darbepoetin-alpha in acute liver failure of mice. Am J Pathol 170:1954–1963. https://doi.org/10.2353/ajpath.2007.061056
54. Williams CD, Bajt ML, Farhood A, Jaeschke H (2010) Acetaminophen-induced hepatic neutrophil accumulation and inflammatory liver injury in CD18-deficient mice. Liver Int 30:1280–1292. https://doi.org/10.1111/j.1478-3231.2010.02284.x
55. James LP, McCullough SS, Knight TR et al (2003) Acetaminophen toxicity in mice lacking NADPH oxidase activity: role of peroxynitrite formation and mitochondrial oxidant stress. Free Radic Res 37:1289–1297
56. Jaeschke H, Williams CD, Ramachandran A, Bajt ML (2012) Acetaminophen hepatotoxicity and repair: the role of sterile inflammation and innate immunity. Liver Int 32:8–20. https://doi.org/10.1111/j.1478-3231.2011.02501.x
57. Laskin DL (2009) Macrophages and inflammatory mediators in chemical toxicity: a battle of forces. Chem Res Toxicol 22:1376–1385. https://doi.org/10.1021/tx900086v
58. Thiel K, Klingert W, Klingert K et al (2017) Porcine model characterizing various parameters assessing the outcome after acetaminophen intoxication induced acute liver failure. World J Gastroenterol 23:1576–1585. https://doi.org/10.3748/wjg.v23.i9.1576
59. Jaeschke H, Lemasters JJ (2003) Apoptosis versus oncotic necrosis in hepatic ischemia/reperfusion injury. Gastroenterology 125:1246–1257

60. Gujral JS, Knight TR, Farhood A et al (2002) Mode of cell death after acetaminophen overdose in mice: apoptosis or oncotic necrosis? Toxicol Sci 67:322–328
61. Kon K, Kim J-S, Jaeschke H, Lemasters JJ (2004) Mitochondrial permeability transition in acetaminophen-induced necrosis and apoptosis of cultured mouse hepatocytes. Hepatology 40:1170–1179. https://doi.org/10.1002/hep.20437
62. Jaeschke H, Cover C, Bajt ML (2006) Role of caspases in acetaminophen-induced liver injury. Life Sci 78:1670–1676. https://doi.org/10.1016/j.lfs.2005.07.003
63. Green DR (2004) The pathophysiology of mitochondrial cell death. Science 305:626–629. https://doi.org/10.1126/science.1099320
64. Mohar et al (2014) Acetaminophen-induced liver damage in mice is associated with gender-specific adduction of peroxiredoxin-6. Redox Biol 2:377–387
65. Lawson JA, Fisher MA, Simmons CA et al (1999) Inhibition of Fas receptor (CD95)-induced hepatic caspase activation and apoptosis by acetaminophen in mice. Toxicol Appl Pharmacol 156:179–186. https://doi.org/10.1006/taap.1999.8635
66. Vollmar B, Menger MD (2009) The hepatic microcirculation: mechanistic contributions and therapeutic targets in liver injury and repair. Physiol Rev 89:1269–1339. https://doi.org/10.1152/physrev.00027.2008
67. Karch J, Kwong JQ, Burr AR et al (2013) Bax and Bak function as the outer membrane component of the mitochondrial permeability pore in regulating necrotic cell death in mice. Elife 2:e00772. https://doi.org/10.7554/eLife.00772
68. Irrinki KM, Mallilankaraman K, Thapa RJ et al (2011) Requirement of FADD, NEMO, and BAX/BAK for aberrant mitochondrial function in tumor necrosis factor alpha-induced necrosis. Mol Cell Biol 31:3745–3758. https://doi.org/10.1128/MCB.05303-11
69. Whelan RS, Konstantinidis K, Wei A-C et al (2012) Bax regulates primary necrosis through mitochondrial dynamics. Proc Natl Acad Sci USA 109:6566–6571. https://doi.org/10.1073/pnas.1201608109
70. Nikam RR, Gore KR (2018) Journey of siRNA: clinical developments and targeted delivery. Nucleic Acid Ther 28:209–224. https://doi.org/10.1089/nat.2017.0715
71. Kulkarni JA, Cullis PR, van der Meel R (2018) Lipid nanoparticles enabling gene therapies: from concepts to clinical utility. Nucleic Acid Ther 28:146–157. https://doi.org/10.1089/nat.2018.0721
72. Setten RL, Rossi JJ, Han S-P (2019) The current state and future directions of RNAi-based therapeutics. Nat Rev Drug Discov 391:806. https://doi.org/10.1038/s41573-019-0017-4
73. Springer AD, Dowdy SF (2018) GalNAc-siRNA conjugates: leading the way for delivery of RNAi therapeutics. Nucleic Acid Ther 28:109–118. https://doi.org/10.1089/nat.2018.0736
74. Huang W, Liang Y, Sang C et al (2018) Therapeutic nanosystems co-deliver anticancer drugs and oncogene SiRNA to achieve synergetic precise cancer chemo-gene therapy. J Mater Chem B 6:3013–3022. https://doi.org/10.1039/C8TB00004B
75. Bajt ML, Knight TR, Lemasters JJ, Jaeschke H (2004) Acetaminophen-induced oxidant stress and cell injury in cultured mouse hepatocytes: protection by N-acetyl cysteine. Toxicol Sci 80:343–349. https://doi.org/10.1093/toxsci/kfh151